

See discussions, stats, and author profiles for this publication at: <https://www.researchgate.net/publication/259498934>

# Development and biological evaluation of Tc-99m-sulfonamide derivatives for in vivo visualization of CA IX as surrogate tumor hypoxia markers

ARTICLE *in* EUROPEAN JOURNAL OF MEDICINAL CHEMISTRY · OCTOBER 2013

Impact Factor: 3.45 · DOI: 10.1016/j.ejmech.2013.10.027 · Source: PubMed

CITATIONS

6

READS

72

## 11 AUTHORS, INCLUDING:



Vamsidhar Akurathi

4 PUBLICATIONS 51 CITATIONS

SEE PROFILE



Ludwig Dubois

Maastricht University

90 PUBLICATIONS 1,472 CITATIONS

SEE PROFILE



Bernard J Cleynhens

University of Leuven

40 PUBLICATIONS 390 CITATIONS

SEE PROFILE



Alfons M Verbruggen

University of Leuven

86 PUBLICATIONS 1,534 CITATIONS

SEE PROFILE



## Original article

Development and biological evaluation of  $^{99m}\text{Tc}$ -sulfonamide derivatives for *in vivo* visualization of CA IX as surrogate tumor hypoxia markers

Vamsidhar Akurathi<sup>a</sup>, Ludwig Dubois<sup>b</sup>, Sofie Celen<sup>a</sup>, Natasja G. Lieuwes<sup>b</sup>,  
Satish K. Chitneni<sup>a</sup>, Bernard J. Cleynhens<sup>a</sup>, Alessio Innocenti<sup>c</sup>, Claudiu T. Supuran<sup>c</sup>,  
Alfons M. Verbruggen<sup>a</sup>, Philippe Lambin<sup>b</sup>, Guy M. Bormans<sup>a,\*</sup>

<sup>a</sup> Laboratory of Radiopharmacy, KU Leuven, Leuven, Belgium

<sup>b</sup> Department of Radiation Oncology (Maastricht Lab), GROW – School for Oncology and Development Oncology, Maastricht University Medical Centre, Maastricht, The Netherlands

<sup>c</sup> Università degli Studi di Firenze, Laboratorio di Chimica Bioinorganica, Room 188, Via della Lastruccia 3, I-50019 Sesto Fiorentino, Firenze, Italy

## ARTICLE INFO

## Article history:

Received 9 July 2013

Received in revised form

8 October 2013

Accepted 10 October 2013

Available online 30 October 2013

## Keywords:

Carbonic anhydrases

Sulfonamides

Technetium-99m

Rhenium

Biodistribution

## ABSTRACT

*In vivo* visualization of tumor hypoxia related markers, such as the endogenous transmembrane protein CA IX may lead to novel therapeutic and diagnostic applications in the management of solid tumors. In this study 4-(2-aminoethyl)benzene sulfonamide (AEBS,  $K_i = 33$  nM for CA IX) has been conjugated with bis(aminoethanethiol) (BAT) and mercaptoacetyldiglycine (MAG<sub>2</sub>) tetradentate ligands and the conjugates radiolabelled with  $^{99m}\text{Tc}$ , to obtain anionic and neutral  $^{99m}\text{Tc}$ -labeled sulfonamide derivatives, respectively. The corresponding rhenium analogues were also prepared and showed good inhibitory activities against hCA IX ( $K_i = 59$ – $66$  nM). In addition, a second generation bis AEBS was conjugated with MAG<sub>2</sub> and labeled with  $^{99m}\text{Tc}$ , and the obtained diastereomers were also evaluated in targeting CA IX. Biodistribution studies in mice bearing HT-29 colorectal xenografts revealed a maximum tumor uptake of  $<0.5\%$  ID/g at 0.5 h p.i. for all the tracers. *In vivo* radiometabolite analysis indicated that at 1 h p.i. MAG<sub>2</sub> tetradentate ligands were more stable in plasma ( $>50\%$  intact) compared to the neutral complex (28% intact). This preliminary data suggest that negatively charged  $^{99m}\text{Tc}$ -labeled sulfonamide derivatives with modest lipophilicity and longer circulation time could be promising markers to target CA IX.

© 2013 Elsevier Masson SAS. All rights reserved.

## 1. Introduction

Carbonic anhydrase (CA) type IX, a transmembrane protein belonging to the class of zinc metalloenzymes, has been identified to play a key role in the extracellular acidification of hypoxic tumors, due to the hypoxia inducing factor (HIF-1) dependent over expression [1]. A low extracellular pH ( $\text{pH}_e$  in hypoxic solid tumors ( $\text{pH}$  6–6.5), in contrast to normal tissue ( $\text{pH}$  7.4), is associated with tumorigenic transformation, chromosomal rearrangements, migration, invasion and overall tumor survival [2–4]. The unique feature of CA IX lies in its expression, where a limited expression in the gastro-intestinal tract is observed in contrast to over expression in carcinomas of kidney, lung, breast, bladder, uterus, cervix, head

and neck [5–10]. The expression of CA IX in these tumors typically varies from 16 to 100% in ‘perinecrotic’ regions and is consistent with the distribution of hypoxia [11]. In addition, the clinical co-relevance of metastasis, poor prognosis and resistance to chemo- and radiotherapy makes CA IX a promising surrogate marker for tumor hypoxia [12–16]. Recent studies from Divgi et al. reported that iodine-124 labeled mAb-cG250, a chimeric monoclonal antibody, effectively recognizes CA IX and provides excellent *in vivo* visualization of clear cell renal cell carcinoma (ccRCC) in a preliminary clinical study. Based on this study, advanced clinical trials are currently underway for application of  $^{124}\text{I}$ -mAb-cG250 in the diagnosis of ccRCC [17].

However, one of the limitations of  $^{124}\text{I}$ -mAb-cG250 is the fact that no discrimination can be made between hypoxic and aerobic cells expressing CA IX, since the antibody binding persists in re-oxygenated tumor cells due to the slow turnover of CA IX (half-life of CA IX upon re-oxygenation is 38 h) and this precludes imaging of periodic or cyclic areas of tumor oxygenation. On the other

\* Corresponding author. O&N2, Bus 821, Herestraat 49, BE-3000 Leuven, Belgium.  
Tel.: +32 16 330447; fax: +32 16 330449.

E-mail address: [guy.bormans@pharm.kuleuven.be](mailto:guy.bormans@pharm.kuleuven.be) (G.M. Bormans).

hand, slower pharmacokinetics of  $^{124}\text{I}$ -mAb-cG50 further confine the imaging protocols for more than six days to obtain a good contrast image, which is a set-back in diagnostic nuclear medicine. Various sulfonamide derivatives with high affinity and selectivity for CA IX and with favourable pharmacokinetics have been reported in literature [12,18]. Studies from Dubois et al. demonstrated that the CA IX active site is accessible for sulfonamides only under hypoxic conditions. Thus, radiolabelled sulfonamides may provide a powerful tool to visualize hypoxic tumors and a promising approach to patient selection for CA IX-directed *in vivo* imaging or therapies based on a functional inhibition of CA IX [19].

In previous work we reported the preparation of  $^{99\text{m}}\text{Tc}(\text{CO})_3$  labeled 4-(2-aminoethyl)benzene-sulfonamide ( $K_i = 33 \text{ nM}$  for CA IX) conjugated with an N-(2-picolyl-amine)-N-acetic acid moiety with reliable (radio)chemical yield and purity. Its rhenium analog was also prepared and showed a  $K_i = 58 \text{ nM}$  for CA IX. Although *in vitro* studies had shown some interesting properties in targeting CA IX, *in vivo* studies revealed that the tracer agent retention in tumor is minimal ( $<0.2\%$  I.D/g at 0.5 h p.i.) in HT 29 colorectal xenograft bearing mice. This low retention in the tumor is attributed to a quick wash out from the blood pool [20]. Studies from Dubois et al. and Supuran et al. demonstrated that charged sulfonamide derivatives have interesting properties with selective inhibition of membrane bound CA IX over the cytosolic isoform [1,19,21]. In a recent study of Lu et al. [22] a series of novel  $\text{Re}/^{99\text{m}}\text{Tc}$ -labelled benzene sulfonate carbonic anhydrase IX inhibitors were synthesized and evaluated for molecular imaging of tumor hypoxia. In their tests they found that the *in vitro* binding affinity of the benzenesulfonamide rhenium complexes yielded  $\text{IC}_{50}$  values ranging from 3 to 116 nM in hypoxic CA-IX expressing HeLa cells. One of the most potent compounds ( $\text{IC}_{50} = 9 \text{ nM}$ ) was radiolabelled with  $^{99\text{m}}\text{Tc}(\text{CO})_3^+$  to afford a technetium-99m-tricarbonyl compound in excellent yield and high purity (Fig. 1). The new compound showed specific binding to CA-IX expressing hypoxic HeLa cells, but no biodistribution data in normal mice or mice bearing a CA-IX expressing tumor were given.

Therefore, it is interesting to develop and evaluate  $^{99\text{m}}\text{Tc}$  labeled sulfonamide derivatives with varying physicochemical properties (Log *D*, complexes with neutral or anionic charge and with variation of molecular mass). The main objective of this study was to explore whether favorable results are obtained with a lipophilic neutral  $^{99\text{m}}\text{Tc}$ -labeled sulfonamide derivative, which is presumed to result in a reservoir-binding of the tracer in blood pool through intracellular erythrocyte CAII binding to maintain an effective

concentration at the target site. On the other hand the presence of a negative charge on a  $^{99\text{m}}\text{Tc}$ -labeled sulfonamide conjugate (anionic complex) could prevent intracellular binding of the tracer agent to other CA subtypes, thereby enhancing the specificity of interaction with membrane bound CA IX. In addition, a second generation anionic  $^{99\text{m}}\text{Tc}$ -labeled bis-sulfonamide derivative was developed, formed as two diastereomers after labeling with  $^{99\text{m}}\text{Tc}$ . A recent report from Morsy et al. further demonstrated that the presence of two sulfonamide moieties can result in increased affinity for the active site of CA IX [21]. Biodistribution characteristics of all the tracer agents synthesized were evaluated in nude mice bearing HT-29 colorectal xenografts for their potential in SPECT imaging.

## 2. Results and discussion

### 2.1. Chemistry and radiolabelling of AEBS-BAT

The precursors used for radiolabeling are all derivatives of AEBS conjugated either to a BAT or a  $\text{MAG}_2$  ligand. The rationale behind choosing BAT or  $\text{MAG}_2$  tetradentate ligands as the  $^{99\text{m}}\text{Tc}$  chelating moiety lies in their ability to form chemically robust core structures. The BAT ligand (**1**) was prepared as reported previously by our group [22]. The two thiol groups of the BAT ligand were each protected by a trityl group to prevent oxidation. One of the secondary amines was protected with a BOC group and the other amine was derivatized with an acetic acid group allowing conjugation with AEBS. The labeling of AEBS-BAT with  $^{99\text{m}}\text{Tc}$  was achieved in a two-step one-pot reaction (Scheme 1). In a first step, the trityl and BOC groups of the BAT ligand were removed by heating **2** at  $100^\circ\text{C}$  for 20 min under acidic conditions. In a second step a cocktail solution of buffering and chelating agents together with stannous ions and  $^{99\text{m}}\text{TcO}_4^-$  was added. Heating of this reaction mixture at  $100^\circ\text{C}$  for 10 min resulted in the formation of a neutral  $^{99\text{m}}\text{Tc}$ -**3** complex. Complex formation involves coordination of  $^{99\text{m}}\text{Tc}$  with the 2 thiol and 2 amine functional groups, to form a stable technetium(V)oxo core [24]. The crude reaction mixture was purified by RP-HPLC with a radiochemical yield of 40% and a radiochemical purity of  $\geq 98\%$  ( $n = 3$ ). The corresponding rhenium analog **Re-3** was synthesized in a low yield (7%) by deprotection of precursor **2** followed by a complexation reaction with the use of  $\text{TBA}[\text{ReOCl}_4]$  [23]. Radio-LC–MS was performed to confirm the identity of  $^{99\text{m}}\text{Tc}$ -**3**. Due to the minute amounts of technetium-99m in the preparation (typically in nano to picomolar range), it is difficult to obtain useful mass spectra of technetium-99m labeled compounds in no-carrier-added form. Therefore, the labeling reaction was done after spiking with technetium-99 ( $\beta^-$  emitter with a half life of  $2.14 \times 10^5$  years) in the form of ammonium pertechnetate and the reaction mixture was analyzed by radio-LC–MS. Fig. 2: depicts a single ion mass chromatogram of  $^{99\text{m}}\text{Tc}$ -**3** and  $^{99\text{m}}\text{Tc}$ -**3** in radiometric channel, supporting the identity of  $^{99\text{m}}\text{Tc}$ -**3**.

### 2.2. Chemistry and radiolabelling of AEBS-MAG<sub>2</sub>

The synthesis of AEBS-MAG<sub>2</sub> (**5**) and subsequent radiolabeling with  $^{99\text{m}}\text{TcO}_4^-$  was carried out as outlined in Scheme 2a, starting from the S-benzyl MAG<sub>2</sub> ligand (**4**). The conjugation with AEBS was accomplished in moderate yields via an amide coupling between the carboxylic acid of MAG<sub>2</sub> and the aminoethyl function of AEBS using a standard peptide coupling agent. The radiolabelling of this conjugate with  $^{99\text{m}}\text{Tc}$  was performed by a classical one-pot exchange labeling reaction. In brief, the deprotection (removal of the S-benzyl group) of precursor (**5**) and the exchange labeling with  $^{99\text{m}}\text{TcO}_4^-$  were carried out in the presence of  $\text{SnCl}_2 \cdot 2\text{H}_2\text{O}$  and chelating agents at  $100^\circ\text{C}$  for 15 min, leading to the anionic complex  $^{99\text{m}}\text{Tc}$ -**8**. The negative charge is due to the coordination of 1

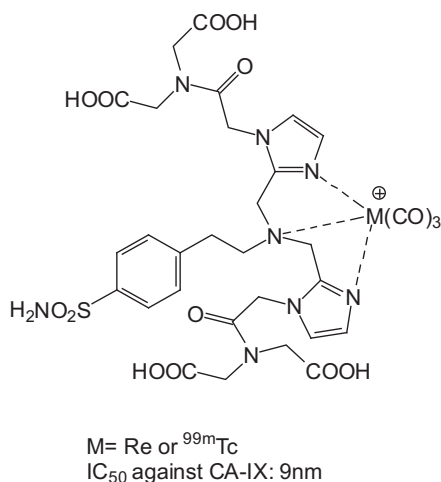
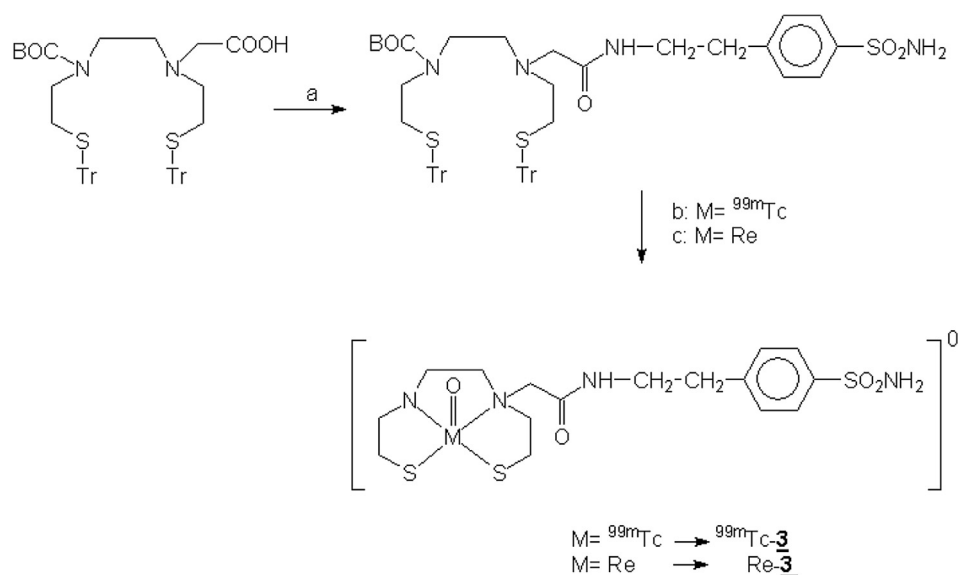


Fig. 1. Structure of the radiolabelled technetium/rhenium tricarbonyl compound evaluated by the group of Lu.



**Scheme 1.** Synthesis of  ${}^{99\text{m}}\text{Tc}$  or Re-labelled **3**. Reagents and conditions: (a) AEBS, dimethylformamide (DMF), dimethylaminopyridine (DMAP), benzotriazol-1-yl-oxy-tripyrrolidinophosphonium hexafluorophosphate (PyBOP) at room temperature (RT) for 4 days (b) (i) TBA[ReOCl<sub>4</sub>], ethanol, HCl gas, 2 h, RT (ii) Et<sub>3</sub>N 0 °C for 12 h (c) HCl 0.5 M, 100 °C for 20 min, Na<sub>2</sub>EDTA 0.1 M, SnCl<sub>2</sub>,  ${}^{99\text{m}}\text{TcO}_4^-$ , 100 °C for 10 min.

thiol and 3 amide functional groups with  ${}^{99\text{m}}\text{Tc}$ , to form a stable technetium(V)oxo core [28]. The crude reaction mixture was purified using RP-HPLC and  ${}^{99\text{m}}\text{Tc-8}$  was obtained with an overall radiochemical yield of 65% and a radiochemical purity of  $\geq 98\%$  ( $n = 3$ ).

The corresponding rhenium analog Re-**8** was synthesized in 3 steps (Scheme 2b). Starting from S-benzoyl protected MAG<sub>2</sub> (**6**)

followed by conjugation with AEBS, S-benzoyl-MAG<sub>2</sub>-AEBS (**7**) was formed in a good yield. The thiol protecting benzoyl group was removed in alkaline conditions, followed by the reaction with a rhenium(V)citrate solution. Re-**8** was isolated from the reaction mixture as the tetraphenyl arsonium chloride salt with a chemical yield of 60%. The identity of  ${}^{99\text{m}}\text{Tc-3}$  was supported by co-elution with Re-**3** (Fig. 3). To synthesise a derivative with two AEBS

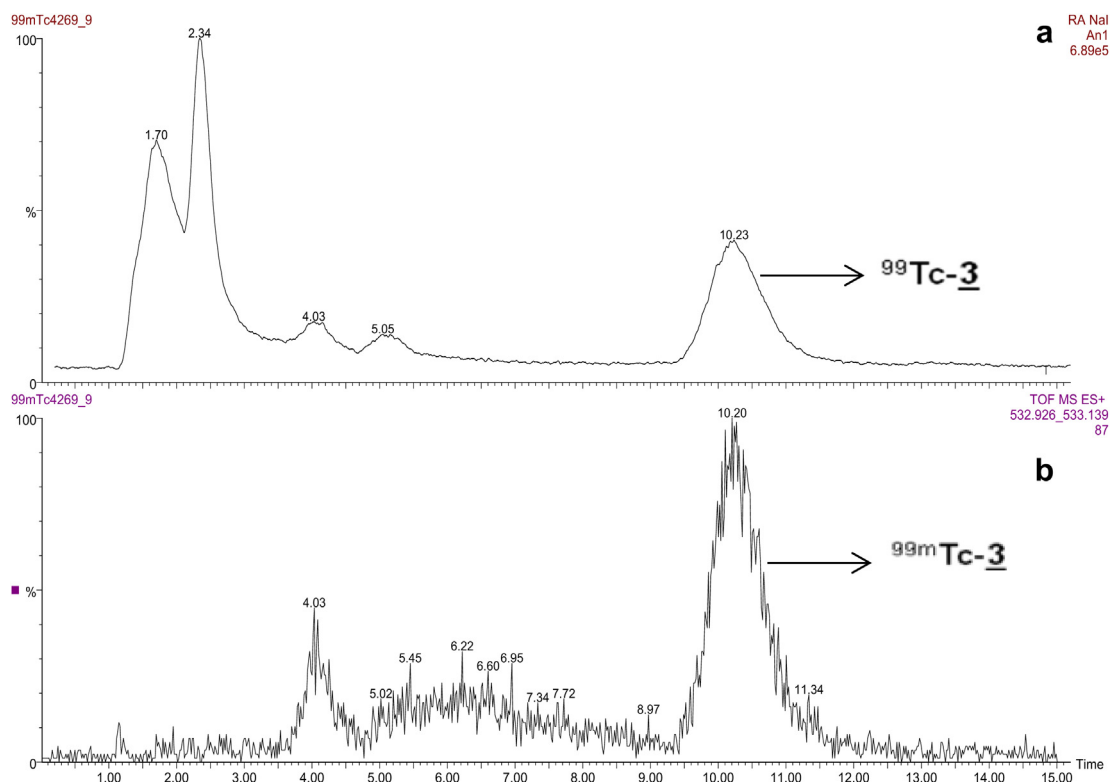
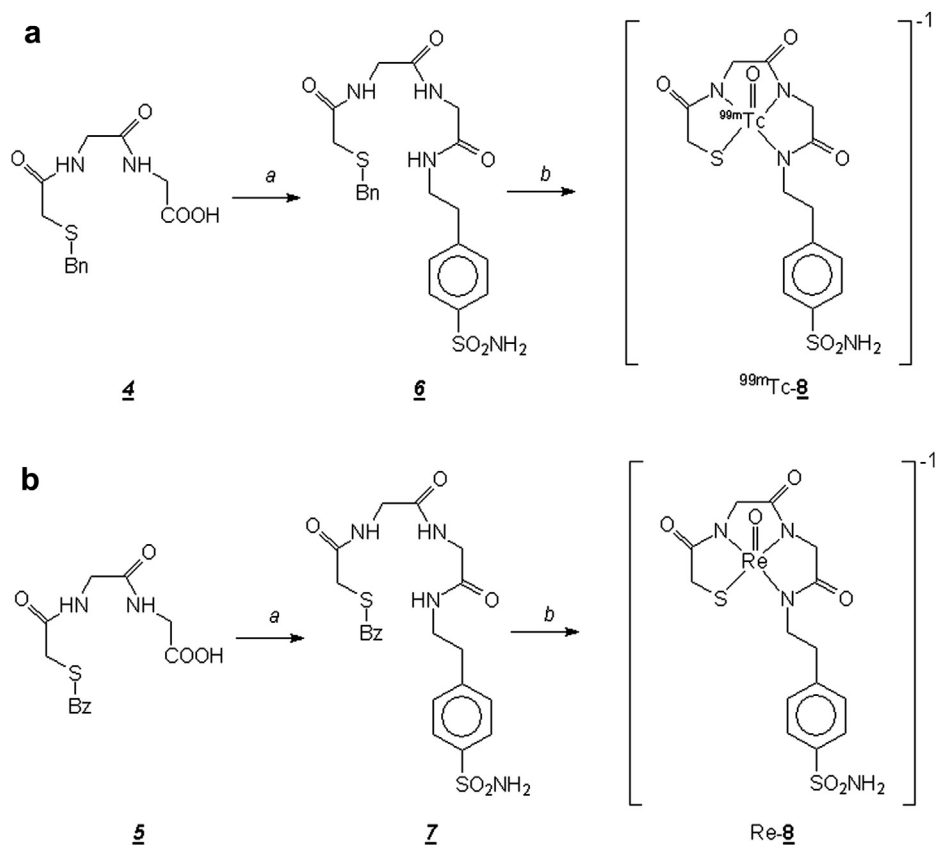


**Fig. 2.** (a) Single ion mass chromatogram of carrier added  ${}^{99\text{m}}\text{Tc-3}$  and (b)  ${}^{99\text{m}}\text{Tc-3}$  in radiometric channel, eluting with a similar retention time of 10.2 min ( $\text{ES}^+$  533.0167 and 533.0173 Da respectively) supporting the identity of  ${}^{99\text{m}}\text{Tc-3}$ .



**Scheme 2.** a. Synthesis of  $^{99m}\text{Tc-8}$ . Reagents and conditions: (a) AEBS, DMF, DMAP and PyBOP at RT for 16 h, 2 M HCl (b) NaK tartrate,  $\text{SnCl}_2$ ,  $^{99m}\text{TcO}_4^-$  at pH 8, 100 °C for 15 min b. Synthesis of Re-8. Reagents and conditions: (a) AEBS, DMF, DMAP and PyBOP at RT for 16 h, 2 M HCl (b) 0.1 M NaOH, 90 °C for 10 min, rhenium(V)citrate solution, 90 °C for 60 min.

moieties, a glutamine spacer (glu) was introduced (Scheme 3). First N-BOC-L-Glu was reacted with two molecules of AEBS followed by deprotection of the amine with TFA. Coupling to the S-benzoyl  $\text{MAG}_2$  precursor (**6**) was done in the same conditions as for the synthesis of **7** with a yield of 55%. The radiolabelling of the conjugate was carried out by a classical one pot exchange reaction followed by purification

with RP-HPLC. Because of the chiral carbon atom in the glutamic acid spacer and due to the syn and anti orientation of the  $^{99m}\text{Tc}=\text{O}$  group, two diastereomers  $^{99m}\text{Tc-11A}$  and  $^{99m}\text{Tc-11B}$  were formed with a radiochemical yield of 52% and 36%, respectively (Fig. 4). Attempts to make the oxo rhenium (V) reference compounds of  $^{99m}\text{Tc-11A}$  and  $^{99m}\text{Tc-11B}$  were not successful.

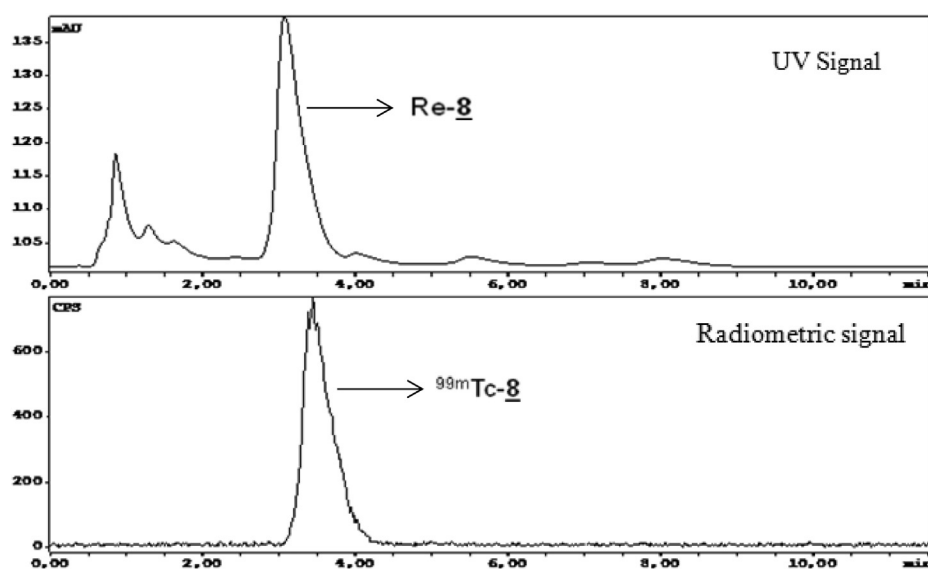
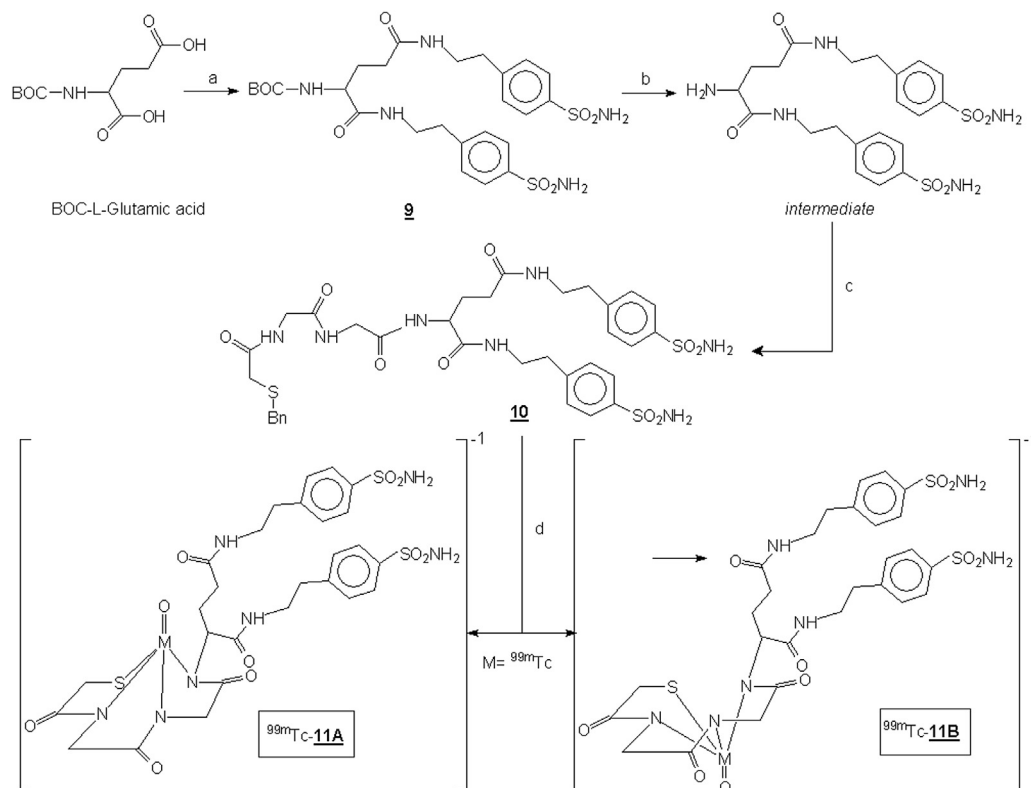


**Fig. 3.** Analytical RP-HPLC chromatogram showing the co-elution of  $^{99m}\text{Tc-8}$  with the Re-8 at about 4 min, supports the identity of  $^{99m}\text{Tc-8}$ .



**Scheme 3.** Synthesis of the diastereomers of  $^{99m}\text{Tc}$ -**11**. Reagents and conditions: (a) AEBS, acetonitrile, 1-(3-dimethylaminopropyl)-3-ethylcarbodiimide HCl (b) trifluoroacetic acid (c)  $\text{MAG}_2$ , DMF, 4-dimethylaminopyrimidine, PyBOP at RT for 16 h (d) NaK tartrate,  $\text{SnCl}_2$  and  $^{99m}\text{TcO}_4^-$  at pH 8, 100 °C for 15 min.

### 2.3. Log *D* and inhibition studies (determination of *K<sub>i</sub>*)

The log *D* is a very useful parameter that can be used to understand the behavior of drug molecules and predict the distribution of a drug compound in a biological system [23]. By a shake flask method, log *D* (1-octanol/phosphate buffer pH 7.4) of the tracer agents  $^{99m}\text{Tc}$ -**3**,  $^{99m}\text{Tc}$ -**8** and  $^{99m}\text{Tc}$ -**11A/B** was  $1.0 \pm 0.02$ ,  $0.5 \pm 0.02$  and  $-1 \pm 0.07$  (mean  $\pm$  S.D,  $n = 6$ ), respectively, indicating that the tracer agents  $^{99m}\text{Tc}$ -**3** and  $^{99m}\text{Tc}$ -**8** are modest in lipophilicity, and the diastereomers  $^{99m}\text{Tc}$ -**11A** and  $^{99m}\text{Tc}$ -**11B** are hydrophilic in nature. The inhibition of the catalytically active and physiologically relevant hCA I, II, IX and XII by the corresponding rhenium analogs Re-**3** and Re-**8** was studied by assaying the CA-catalyzed  $\text{CO}_2$  hydration activity [24]. The inhibition activity (*K<sub>i</sub>*) against hCA IX was found to be 59 nM for Re-**3** and 66 nM for Re-**8** (Table 1). Despite the presence of a bulky chelating group (BAT or  $\text{MAG}_2$ ), the rhenium

**Table 1**

Inhibition constants of reference compounds Re-**3**, Re-**8** and AEBS against carbonic anhydrase isozymes hCA I, II, IX and XII for the  $\text{CO}_2$  hydration reaction at 25 °C.

Compound	hCA I <sup>b</sup>	hCA II <sup>b</sup>	<i>K<sub>i</sub></i> (nM) <sup>a</sup>	hCA XII <sup>b</sup>	Selectivity ratio
			hCA IX <sup>b</sup>		hCA II/IX <sup>c</sup>
Re- <b>3</b>	268	165	59	76	2.8
Re- <b>8</b>	4875	47	66	57	0.7
AEBS	2100	160	33	3.2	4.8

<sup>a</sup> Standard errors of the mean in the range of 5–10% of the reported value ( $n = 3$ , different assays).

<sup>b</sup> h – Human (cloned) isozymes<sup>41</sup>.

<sup>c</sup> *K<sub>i</sub>* ratios are indicative of selectivity.

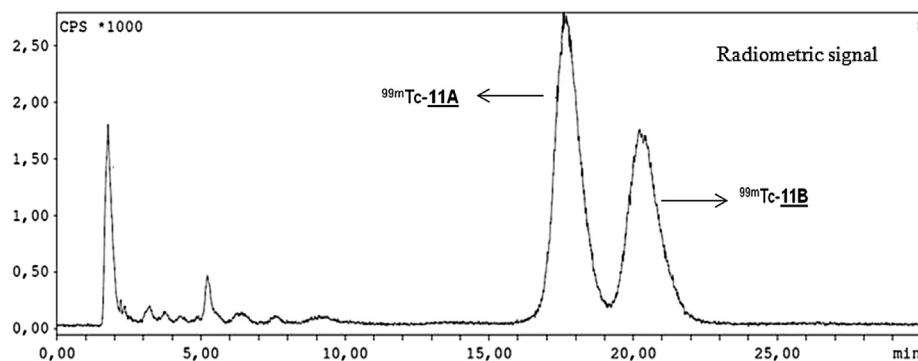


**Fig. 4.** Semipreparative RP-HPLC chromatogram showing diastereomers of  $^{99m}\text{Tc}$ -**11A** and **11B** eluting at about 18 min and 21 min, respectively.



analogs show a good inhibitory activity, comparable to that of the parent moiety AEBS ( $K_i = 33$  nM). The selectivity ratios of the rhenium analogs for CA IX over cytosolic isoforms of hCA II were found to be modest when compared to the parent moiety.

#### 2.4. *In vivo* studies

The biodistribution data of  $^{99m}\text{Tc-3}$ ,  $^{99m}\text{Tc-8}$  and diastereomers  $^{99m}\text{Tc-11A}$  and  $^{99m}\text{Tc-11B}$  in CA IX expressing HT 29 colorectal xenograft mice are summarized in Tables 2 and 3, respectively. Data are expressed as percentage of the injected dose (% ID) and percentage of the injected dose per gram of tissue (% ID/g) for selected body parts. All tracer agents were cleared mainly via the hepatobiliary pathway with  $\geq 70\%$  of the ID in intestines at 4 h p.i. A smaller fraction was cleared via the renal pathway ( $\leq 19\%$  ID in urine at 4 h p.i.). Surprisingly, the clearance of diastereomers  $^{99m}\text{Tc-11A}$  and  $^{99m}\text{Tc-11B}$  occurred also via the hepatobiliary pathway despite of their negative charge. Polar compounds bearing a negative charge are considered to be hydrophilic in nature and expected to clear more via the renal pathway [30].

The retention of the tracer agents  $^{99m}\text{Tc-3}$ ,  $^{99m}\text{Tc-8}$  and  $^{99m}\text{Tc-11A}$  and  $^{99m}\text{Tc-11B}$  in the blood pool was about 13%, 1.5% and 0.1% ID at 0.5 h p.i., respectively, indicating the strategy to attain high concentration of  $^{99m}\text{Tc-3}$  in blood pool was accomplished with 10–130 fold higher retention in the blood pool, when compared to  $^{99m}\text{Tc-8}$  and diastereomers of  $^{99m}\text{Tc-11A}$  and  $^{99m}\text{Tc-11B}$  complexes. *In vitro* incubation studies performed on human whole blood with  $^{99m}\text{Tc-3}$  showed that about 13% of activity was retained in RBCs after 10 min incubation at RT (data not shown). Thus, the higher activity in the blood pool associated with tracer  $^{99m}\text{Tc-3}$  is due to diffusion through RBC membrane and subsequent interaction with the CA II isozyme located in erythrocytes [9–12]. The tracer agents  $^{99m}\text{Tc-8}$  and diastereomers  $^{99m}\text{Tc-11A}$  and  $^{99m}\text{Tc-11B}$  are presumably confined to the extracellular space due to their anionic charge.

All other organs (spleen, pancreas, lungs, heart and brain) showed negligible tracer retention, similar to the previously reported  $^{99m}\text{Tc}(\text{CO})_3$  labeled AEBS [24]. The concentration of tracer  $^{99m}\text{Tc-3}$  in the tumors was found to be  $\leq 0.2\%$  ID/g, for  $^{99m}\text{Tc-}$

**Table 2b**

Biodistribution of  $^{99m}\text{Tc-8}$  in CA IX expressing tumor bearing mice at 0.5, 1, 2 and 4 h p.i. Data are expressed as mean  $\pm$  standard error ( $n = 3$ ).

$^{99m}\text{Tc-8}$				
Organs [% ID]	0.5 h	1 h	2 h	4 h
Kidneys	21.6 $\pm$ 3.0	17.5 $\pm$ 2.0	7.2 $\pm$ 3.6	4.4 $\pm$ 0.9
Urine	6.9 $\pm$ 1.8	6.1 $\pm$ 2.6	18.5 $\pm$ 5.0	19.4 $\pm$ 7.0
Liver	38.6 $\pm$ 3.6	35.9 $\pm$ 3.6	18.9 $\pm$ 6.9	12.0 $\pm$ 2.1
Spleen + pancreas	0.1 $\pm$ 0.0	0.1 $\pm$ 0.0	0.1 $\pm$ 0.1	0.0 $\pm$ 0.0
Lungs	0.4 $\pm$ 0.0	0.2 $\pm$ 0.0	0.1 $\pm$ 0.0	0.1 $\pm$ 0.0
Heart	0.1 $\pm$ 0.0	0.0 $\pm$ 0.0	0.0 $\pm$ 0.0	0.0 $\pm$ 0.0
Intestines	23.3 $\pm$ 5.6	35.2 $\pm$ 3.0	52.0 $\pm$ 6.7	62.4 $\pm$ 2.9
Stomach	0.8 $\pm$ 0.1	0.1 $\pm$ 0.1	1.1 $\pm$ 0.5	0.6 $\pm$ 0.2
Brain	0.0 $\pm$ 0.0	0.0 $\pm$ 0.0	0.0 $\pm$ 0.0	0.0 $\pm$ 0.0
Blood	1.5 $\pm$ 0.4	1.1 $\pm$ 0.0	0.8 $\pm$ 0.1	0.5 $\pm$ 0.0
Tumor	0.1 $\pm$ 0.0	0.2 $\pm$ 0.0	0.2 $\pm$ 0.0	0.1 $\pm$ 0.1
$^{99m}\text{Tc-8}$				
Organs [% ID/g]	0.5 h	1 h	2 h	4 h
Kidneys	37.6 $\pm$ 4.1	37.7 $\pm$ 2.4	12.1 $\pm$ 5.2	6.8 $\pm$ 1.4
Liver	17.5 $\pm$ 1.6	17.3 $\pm$ 1.8	7.3 $\pm$ 2.5	5.6 $\pm$ 2.3
Spleen + pancreas	0.2 $\pm$ 0.1	0.2 $\pm$ 0.0	0.2 $\pm$ 0.1	0.1 $\pm$ 0.0
Lungs	0.9 $\pm$ 0.1	0.6 $\pm$ 0.1	0.3 $\pm$ 0.1	0.2 $\pm$ 0.0
Heart	0.4 $\pm$ 0.1	0.3 $\pm$ 0.0	0.1 $\pm$ 0.0	0.1 $\pm$ 0.0
Brain	0.0 $\pm$ 0.0	0.0 $\pm$ 0.0	0.0 $\pm$ 0.0	0.0 $\pm$ 0.0
Blood	1.3 $\pm$ 0.3	0.9 $\pm$ 0.1	0.7 $\pm$ 0.2	0.4 $\pm$ 1.0
Tumor	0.5 $\pm$ 0.1	0.4 $\pm$ 0.0	0.2 $\pm$ 0.0	0.1 $\pm$ 0.0
Tumor/blood	0.4 $\pm$ 0.0	0.4 $\pm$ 0.1	0.3 $\pm$ 0.1	0.5 $\pm$ 0.0

$^{99m}\text{Tc-8}$   $\leq 0.5\%$  ID/g, and for diastereomers  $^{99m}\text{Tc-11A}$  and  $^{99m}\text{Tc-11B}$  a negligible retention of  $\leq 0.2\%$  ID/g in the tumors was observed at 0.5–4 h p.i. indicating that overall retention of these tracer agents in the tumors was minimal.

However, with  $^{99m}\text{Tc-8}$  a 2.5 fold higher retention is observed as compared to the three other radioligands. This slightly higher tumor uptake of  $^{99m}\text{Tc-8}$  can probably be attributed to its interaction with the active site of CA IX in a distinct manner. The anionic charge and the modest lipophilicity associated with this complex presumably restrict the tracer to the extracellular space, thereby promoting its interaction with the active site of CA IX. On the other hand, the diastereomers  $^{99m}\text{Tc-11A}$  and  $^{99m}\text{Tc-11B}$  have a low retention in tumors due to their quick wash out from the blood pool. Further, the tumor to blood ratios with the  $^{99m}\text{Tc-8}$  and the diastereomers  $^{99m}\text{Tc-11A}$  and  $^{99m}\text{Tc-11B}$  has been found to be modest with values ranging from 0.3 to 1 and with  $^{99m}\text{Tc-3}$  it is zero. The polar surface area (PSA), another important parameter that can provide information about the hydrogen bonding capacity of the molecules, was found to be 109 Å<sup>2</sup>, 138 Å<sup>2</sup> for  $^{99m}\text{Tc-3}$  and  $^{99m}\text{Tc-8}$  respectively and for the diastereomers  $^{99m}\text{Tc-11A}$  and  $^{99m}\text{Tc-11B}$  it was 256 Å<sup>2</sup>. Generally a PSA of  $< 60$  Å<sup>2</sup> is considered to be a requirement for an efficient cellular diffusion of a molecule.

This is in line with the higher blood pool retention observed for  $^{99m}\text{Tc-3}$ . Studies from Gidal et al. have shown that erythrocytes play an important role in the circulatory transport of sulfonamide derivatives and extend the *in vivo* half-life of the antiepileptic drugs such as zonisamide and topiramate [25]. Using a similar strategy of erythrocyte mediated carrier to extend the *in vivo* half-life of tracer agent  $^{99m}\text{Tc-3}$  is intriguing. However, the *in vivo* results of  $^{99m}\text{Tc-3}$  indicated a reduced uptake in the tumors.

The reason for the limited tumor retention of  $^{99m}\text{Tc-8}$  is possibly due to its fast elimination during the passage of blood through the metabolising organs such as the liver or due to *in vivo* instability. Further the low perfusion of the hypoxic tumor limits the tracer delivery to the tumor. *Ex vivo* western blot analysis confirmed that the CA IX expression levels of the tumors that were evaluated in biodistribution studies, and the signal intensity was comparable with that in HT-29 cells exposed to hypoxia *in vitro* (Fig. 5).

**Table 2a**

Biodistribution of  $^{99m}\text{Tc-3}$  in CA IX expressing tumor bearing mice at 0.5, 2 and 4 h p.i. Data are expressed as mean  $\pm$  standard error ( $n = 3$ ).

$^{99m}\text{Tc-3}$			
Organs [% ID]	0.5 h	2 h	4 h
Kidneys	8.9 $\pm$ 1.3	1.3 $\pm$ 0.0	0.8 $\pm$ 0.0
Urine	11.4 $\pm$ 0.5	14.9 $\pm$ 1.5	19.4 $\pm$ 4.2
Liver	25.2 $\pm$ 4.8	18.4 $\pm$ 0.3	11.4 $\pm$ 2.1
Spleen + pancreas	0.6 $\pm$ 0.0	0.2 $\pm$ 0.0	0.1 $\pm$ 0.0
Lungs	1.3 $\pm$ 0.1	0.4 $\pm$ 0.1	0.2 $\pm$ 0.1
Heart	0.4 $\pm$ 0.1	0.2 $\pm$ 0.0	0.1 $\pm$ 0.0
Intestines	31.9 $\pm$ 3.7	54.2 $\pm$ 2.5	61.3 $\pm$ 5.5
Stomach	1.6 $\pm$ 0.2	0.8 $\pm$ 0.1	1.0 $\pm$ 0.2
Brain	0.1 $\pm$ 0.0	0.0 $\pm$ 0.0	0.0 $\pm$ 0.0
Blood	12.7 $\pm$ 0.5	8.3 $\pm$ 0.1	3.5 $\pm$ 1.1
Tumor	0.3 $\pm$ 0.0	0.2 $\pm$ 0.0	0.1 $\pm$ 0.0
$^{99m}\text{Tc-3}$			
Organs [% ID/g]	0.5 h	2 h	4 h
Kidneys	15.3 $\pm$ 1.5	2.2 $\pm$ 0.1	1.5 $\pm$ 0.1
Liver	11.6 $\pm$ 2.8	9.8 $\pm$ 0.1	6.8 $\pm$ 1.8
Spleen + pancreas	1.3 $\pm$ 0.1	0.7 $\pm$ 0.1	0.3 $\pm$ 0.0
Lungs	3.7 $\pm$ 0.1	1.6 $\pm$ 0.4	0.8 $\pm$ 0.3
Heart	2.2 $\pm$ 0.6	1.1 $\pm$ 0.2	0.5 $\pm$ 0.1
Brain	0.2 $\pm$ 0.0	0.1 $\pm$ 0.0	0.1 $\pm$ 0.0
Blood	10.7 $\pm$ 2.0	6.8 $\pm$ 0.1	3.4 $\pm$ 1.4
Tumor	0.2 $\pm$ 0.0	0.1 $\pm$ 0.0	0.1 $\pm$ 0.0
Tumor/blood	0.0 $\pm$ 0.0	0.0 $\pm$ 0.0	0.0 $\pm$ 0.0

**Table 3a**

Biodistribution of  $^{99m}\text{Tc}$ -**11A** in CA IX expressing tumor bearing mice at 0.5, 1, 2 and 4 h p.i. Data are expressed as mean  $\pm$  standard error ( $n = 3$ ).

$^{99m}\text{Tc}$ - <b>11A</b>				
Organs [% ID ]	0.5 h	1 h	2 h	4 h
Kidneys	7.8 $\pm$ 0.1	2.6 $\pm$ 1.6	1.5 $\pm$ 0.5	0.2 $\pm$ 0.1
Urine	1.3 $\pm$ 1.0	1.0 $\pm$ 0.6	0.4 $\pm$ 0.3	6.2 $\pm$ 1.2
Liver	28.3 $\pm$ 2.9	8.3 $\pm$ 5.0	8.9 $\pm$ 3.0	14.3 $\pm$ 8.9
Spleen + pancreas	0.1 $\pm$ 0.1	0.1 $\pm$ 0.0	0.1 $\pm$ 0.0	0.0 $\pm$ 0.0
Lungs	0.1 $\pm$ 0.0	0.1 $\pm$ 0.0	0.0 $\pm$ 0.0	0.0 $\pm$ 0.0
Heart	0.1 $\pm$ 0.0	0.1 $\pm$ 0.3	0.0 $\pm$ 0.0	0.0 $\pm$ 0.0
Intestines	57.4 $\pm$ 2.9	80.2 $\pm$ 1.7	85.5 $\pm$ 2.4	78.9 $\pm$ 7.8
Stomach	0.9 $\pm$ 0.1	0.7 $\pm$ 0.6	1.2 $\pm$ 0.7	1.9 $\pm$ 0.4
Brain	0.0 $\pm$ 0.0	0.0 $\pm$ 0.0	0.0 $\pm$ 0.0	0.0 $\pm$ 0.0
Blood	0.1 $\pm$ 0.0	0.1 $\pm$ 0.0	0.1 $\pm$ 0.0	0.1 $\pm$ 0.0
Tumor	0.2 $\pm$ 0.0	0.0 $\pm$ 0.0	0.1 $\pm$ 0.0	0.1 $\pm$ 0.0

$^{99m}\text{Tc}$ - <b>11A</b>				
Organs [% ID/g]	0.5 h	1 h	2 h	4 h
Kidneys	25.5 $\pm$ 6.4	5.8 $\pm$ 4.4	4.6 $\pm$ 1.2	0.4 $\pm$ 0.1
Liver	22.6 $\pm$ 3.6	5.3 $\pm$ 3.3	6.9 $\pm$ 2.3	11.1 $\pm$ 6.8
Spleen + pancreas	0.6 $\pm$ 0.6	0.4 $\pm$ 0.1	0.3 $\pm$ 0.1	0.5 $\pm$ 0.3
Lungs	0.5 $\pm$ 0.1	0.3 $\pm$ 0.2	0.1 $\pm$ 0.0	0.1 $\pm$ 0.1
Heart	1.0 $\pm$ 0.2	0.7 $\pm$ 0.4	0.2 $\pm$ 0.0	0.2 $\pm$ 0.1
Brain	0.0 $\pm$ 0.0	0.0 $\pm$ 0.0	0.0 $\pm$ 0.0	0.0 $\pm$ 0.0
Blood	0.1 $\pm$ 0.0	0.1 $\pm$ 0.0	0.1 $\pm$ 0.0	0.0 $\pm$ 0.0
Tumor	0.1 $\pm$ 0.0	0.1 $\pm$ 0.0	0.0 $\pm$ 0.0	0.1 $\pm$ 0.0
Tumor/blood	1.0 $\pm$ 0.0	1.0 $\pm$ 0.0	0.0 $\pm$ 0.0	0.1 $\pm$ 0.0

Another possible reason for a lower retention of the tracer agents could be a low  $B_{\text{max}}$  (concentration of CA IX in tumor tissue) and  $K_d$  (dissociation constant for the ligand-CA IX complex). Ideally a  $B_{\text{max}}/K_d$  ratio should be  $\geq 2$  for an efficient binding and imaging [26]. Finally, the *in vivo* stability of the new complexes was studied by determination of the percentage of parent tracer in plasma of NMRI mice ( $n = 2$ ) at 1 h p.i. using RP-HPLC. This was 28% for the neutral complex  $^{99m}\text{Tc}$ -**3** and 77% for  $^{99m}\text{Tc}$ -**8** respectively. For the diastereomers  $^{99m}\text{Tc}$ -**11A** and  $^{99m}\text{Tc}$ -**11B** about 65% and 52% was found to be intact, indicating that these anionic complexes were relatively stable when compared to the neutral  $^{99m}\text{Tc}$ -**3** complex.

**Table 3b**

Biodistribution of  $^{99m}\text{Tc}$ -**11B** in CA IX expressing tumor bearing mice at 0.5, 1, 2 and 4 h p.i. Data are expressed as mean  $\pm$  standard error ( $n = 3$ ).

$^{99m}\text{Tc}$ - <b>11B</b>				
Organs [% ID ]	0.5 h	1 h	2 h	4 h
Kidneys	8.1 $\pm$ 1.9	1.3 $\pm$ 0.3	0.5 $\pm$ 0.2	0.0 $\pm$ 0.0
Urine	2.3 $\pm$ 1.4	2.9 $\pm$ 2.0	1.3 $\pm$ 1.0	1.7 $\pm$ 1.4
Liver	28.9 $\pm$ 1.6	12.0 $\pm$ 1.3	15.7 $\pm$ 3.6	2.4 $\pm$ 0.1
Spleen + pancreas	0.1 $\pm$ 0.0	0.1 $\pm$ 0.0	0.1 $\pm$ 0.1	0.0 $\pm$ 0.0
Lungs	0.1 $\pm$ 0.0	0.1 $\pm$ 0.0	0.1 $\pm$ 0.1	0.0 $\pm$ 0.0
Heart	0.0 $\pm$ 0.0	0.0 $\pm$ 0.0	0.0 $\pm$ 0.0	0.0 $\pm$ 0.0
Intestines	55.5 $\pm$ 11.6	62.4 $\pm$ 2.9	78.2 $\pm$ 2.2	94.7 $\pm$ 2.5
Stomach	1.9 $\pm$ 0.4	0.6 $\pm$ 0.2	1.4 $\pm$ 0.8	0.1 $\pm$ 0.0
Brain	0.0 $\pm$ 0.0	0.0 $\pm$ 0.0	0.0 $\pm$ 0.0	0.0 $\pm$ 0.0
Blood	0.1 $\pm$ 0.0	0.5 $\pm$ 0.0	0.1 $\pm$ 0.0	0.0 $\pm$ 0.0
Tumor	0.3 $\pm$ 0.1	0.1 $\pm$ 0.1	0.2 $\pm$ 0.1	0.2 $\pm$ 0.1

$^{99m}\text{Tc}$ - <b>11B</b>				
Organs [% ID/g]	0.5 h	1 h	2 h	4 h
Kidneys	24.0 $\pm$ 5.5	4.4 $\pm$ 0.1	1.8 $\pm$ 0.6	0.1 $\pm$ 0.0
Liver	24.6 $\pm$ 8.6	11.1 $\pm$ 1.7	15.1 $\pm$ 3.7	2.0 $\pm$ 0.8
Spleen + pancreas	0.3 $\pm$ 0.0	0.3 $\pm$ 0.1	0.7 $\pm$ 0.6	0.0 $\pm$ 0.0
Lungs	0.2 $\pm$ 0.1	0.3 $\pm$ 0.1	0.6 $\pm$ 0.5	0.1 $\pm$ 0.1
Heart	0.2 $\pm$ 0.0	0.1 $\pm$ 0.0	0.1 $\pm$ 0.0	0.0 $\pm$ 0.0
Brain	0.0 $\pm$ 0.0	0.0 $\pm$ 0.0	0.0 $\pm$ 0.0	0.0 $\pm$ 0.0
Blood	0.5 $\pm$ 0.1	0.2 $\pm$ 0.0	0.2 $\pm$ 0.0	0.1 $\pm$ 0.1
Tumor	0.1 $\pm$ 0.0	0.2 $\pm$ 0.0	0.2 $\pm$ 0.1	0.1 $\pm$ 0.0
Tumor/blood	0.2 $\pm$ 0.0	1.0 $\pm$ 0.2	1.0 $\pm$ 0.1	1.0 $\pm$ 0.0

On the other hand there was no marked accumulation of tracer agents in the stomach, indicating that there was no free  $^{99m}\text{TcO}_4^-$  present. In addition, the reduced plasma stability of  $^{99m}\text{Tc}$ -**3** could also explain the reduced retention in the tumors.

### 3. Conclusions

The sulfonamide derivative AEBS, an inhibitor for CA IX was conjugated with the BAT and  $\text{MAG}_2$  ligand, and radiolabelled with  $^{99m}\text{Tc}$ . The resulting radiolabelled neutral and anionic complexes were obtained in high radiochemical yields and purity. The corresponding rhenium analogs showed a good inhibitory constant against CA IX. Biodistribution studies in mice bearing HT-29 tumor xenografts revealed a limited retention in tumors ( $\leq 0.5\%$  I.D at 0.5–4 h p.i.) for all tracer agents. The anionic tracer  $^{99m}\text{Tc}$ -**8** showed a modest tracer retention (0.5% I.D/g at 0.5 h), whereas with the diastereomeric bis-sulfonamides complexes  $^{99m}\text{Tc}$ -**11A** and **11B** where a dual interaction with CA IX is anticipated showed low tumor uptake ( $\leq 0.2\%$  I.D/g) primarily due to a fast clearance from the blood pool. The strategy using the blood pool as a reservoir for the sulfonamide derivative  $^{99m}\text{Tc}$ -**3** did not result in an increased retention in the tumor. It is concluded that screening of other sulfonamide derived radiolabelled complexes possessing a charge, a slow clearance, and high affinity and selectivity for CA IX is necessary. This will contribute to the exploration of the potential of CA IX inhibitors in diagnosis and treatment of hypoxic tumors, which are highly non-responsive to classical chemo- and radiotherapy.

### 4. Experimental procedures

#### 4.1. Materials and methods

Reagents and solvents were obtained commercially from Acros (Geel, Belgium), Aldrich, Fluka, Sigma (Sigma-Aldrich, Bornem, Belgium), Merck (Darmstadt, Germany), TCI-Europe (Zwijndrecht, Belgium) or Fischer Bioblock Scientific (Tournai, Belgium) and used without further purification unless otherwise specified.  $^{99m}\text{TcO}_4^-$  was eluted from a  $^{99}\text{Mo}/^{99m}\text{Tc}$  generator (UltraTechnikow<sup>®</sup>, Covidien, Petten, The Netherlands).  $^1\text{H}$  NMR spectra were recorded on a Bruker 400 MHz spectrometer (Brussels, Belgium). Chemical shifts are reported in parts per million (ppm) relative to tetramethylsilane ( $\delta = 0$ ). Coupling constants are reported in hertz (Hz). Splitting patterns are defined by s (singlet), d (doublet), t (triplet) and m (multiplet). HPLC analysis was performed on a LaChrom Elite HPLC system (Hitachi, Darmstadt, Germany) connected to a UV spectrometer set at 254 nm. For analysis of radiolabelled compounds, the HPLC eluate after passage through the UV detector was directed over a 3-inch NaI(Tl) scintillation detector connected to a single channel analyzer (Gabi box, Raytest, Straubenhardt, Germany). System A was equipped with an XTerra analytical C18 column (4.6 mm  $\times$  250 mm, Waters, Milford, MA, USA) eluted in an isocratic way with 0.5 M ammonium acetate pH 6.7: ethanol (60:40 V/V) at a flow rate of 1 mL/min. System B employed an analytical XBridge C18 column (4.6 mm  $\times$  150 mm, Waters) eluted isocratically with a mobile phase consisting of 0.01 M disodium hydrogen phosphate buffer pH 8.0: ethanol (75:25 V/V) at a flow rate of 1 mL/min. System C was equipped with the same column of system B but used an isocratic mobile phase consisting of 0.05 M ammonium acetate buffer pH 6.6: ethanol (82:18 V/V). Combined radioliquid chromatography and mass spectrometry (radio-LC–MS) analysis was performed on a system consisting of a Waters Alliance 2690 separation module connected to an XTerra MS C18 column (3.5  $\mu\text{m}$ , 2.1 mm  $\times$  50 mm; Waters) eluted with gradient mixtures of 0.01% formic acid and acetonitrile (0 min 100:0 V/V, linear gradient for



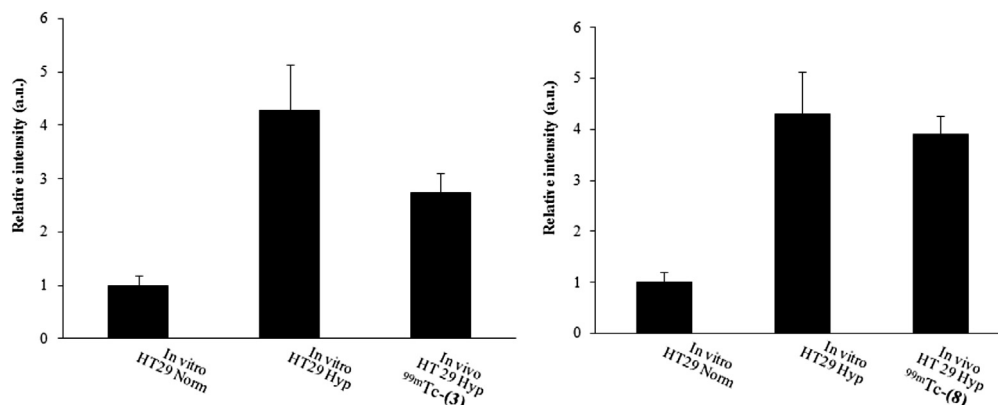


**Fig. 5.** *In vitro* and *in vivo* assessment of CA IX expression in HT-29 cell lines under normoxic and hypoxic (0.2% O<sub>2</sub>) conditions by densitometric analysis of the western blots. Upregulation of CA IX expression was observed in the tumors of mice that were injected with <sup>99m</sup>Tc-3 or <sup>99m</sup>Tc-8.

6 min reaching 50:50 V/V, followed by isocratic elution with 50:50 V/V to 10 min) at a flow rate of 0.2 mL/min. The eluent was monitored for UV absorbance (Waters 2487 Dual wavelength absorbance detector) and radioactivity (3-inch NaI(Tl) detector). The time-of-flight mass spectrometer (Micromass LCT, Manchester, UK) was equipped with an electrospray ionization (ESI) source. Data acquisition and processing was performed with Masslynx software (version 3.5, Waters). Quantification of radioactivity in samples of biodistribution studies and *in vivo* stability analyses was done using an automated gamma counter equipped with a 3-inch NaI(Tl) well crystal coupled to a multichannel analyzer (Wallac 1480 Wizard, Wallac, Turku, Finland). The results were corrected for background radiation and physical decay during counting. The polar surface area (PSA) of the reference compounds is calculated by using Marvin space software from Chemaxon (Budapest, Hungary). All animal experiments were conducted according to the Belgian code of practice for the care and use of animals, after approval from the university ethics committee for animals. The mice were housed in individually ventilated cages in a thermo-regulated (~22 °C), humidity-controlled facility under a 12 h/12 h light/dark cycle with access to food and water *ad libitum*. The CA IX expressing HT-29 tumor cells were cultured as previously described [19]. The HT-29 cells were resuspended in Basement Membrane Matrix (Matrigel™ BD, Biosciences, Breda, The Netherlands) and injected subcutaneously into a lateral flank of the animal. When tumors reached an average volume of 400 mm<sup>3</sup> the animals were used for the biodistribution studies.

## 4.2. Synthesis

### 4.2.1. *S,S'*-bis-triphenylmethyl-*N*-(BOC)-*N'*-(acetic acid)-1,2-ethylenedi-cysteamine (*S,S'*-bis-trityl-*N*-BOC-*N'*-(acetic acid)BAT, **1**)

The title compound was synthesized as previously reported by our group [27] with a yield of 97%. C<sub>51</sub>H<sub>54</sub>N<sub>2</sub>O<sub>4</sub>S<sub>2</sub> ESI-MS: [M + H]<sup>+</sup> calcd 822.3, found 822.5.

### 4.2.2. Conjugation of 4-(2-aminoethyl)benzene sulfonamide (AEBS) with *S,S'*-bis-trityl-*N*-BOC-*N'*-(acetic acid)BAT (**2**)

To a solution of AEBS (0.3 mmol, 60 mg) in DMF (5 mL), DMAP (0.6 mmol, 73 mg), PyBOP (0.6 mmol, 303 mg) and **1** (0.3 mmol, 250 mg) were added and the mixture was stirred at room temperature (RT) for 2 h. DMF was evaporated under reduced pressure, water (50 mL) was added and this solution was extracted twice with CH<sub>2</sub>Cl<sub>2</sub> (2 × 50 mL). The organic phases were combined, washed with water and brine, dried using MgSO<sub>4</sub> and evaporated under reduced pressure. The residue was purified using silica gel

column chromatography with gradient mixtures of dichloromethane and methanol (100:0 to 95:5). The purified product was obtained as white foam with a yield of 66% (0.2 mmol, 200 mg). C<sub>59</sub>H<sub>64</sub>N<sub>4</sub>O<sub>5</sub>S<sub>3</sub> ESI-MS: [M + H]<sup>+</sup> calcd 1004.4, found 1004.4. <sup>1</sup>H NMR, 400 MHz (DMSO -d<sub>6</sub>) δ 7.19–7.29 (m, 34H), 2.87 (t, 4H), 2.80 (s, 2H), 2.77 (s, 2H), 2.67–2.71 (m, 4H, *J* = 8.10), 2.31 (t, 2H), 2.2 (t, 4H), 1.2 (s, 9H).

### 4.2.3. Synthesis of complex of **2** with rhenium (**Re-3**)

The formation of the complex of rhenium with the BAT analogue **2** proceeded in two steps. In a first step the precursor TBA[ReOCl<sub>4</sub>] was synthesized as reported earlier [28]. Briefly, under stirring, HCl gas was bubbled slowly through a solution of TBA[ReO<sub>4</sub>] (tetrabutylammonium perrhenate, 2.2 mmol, 1.1 g) in ethanol (20 mL). The solution initially turned to an intense yellow color. Addition of HCl was continued until complete saturation, observed by a change of the color to dark yellow. The volume of the solution was reduced to 50% with a stream of nitrogen. The precursor crystallized out after 12 h at 0 °C and was filtered off. Yield 60 mg (0.1 mmol, 5%). In a second step, the protecting groups of the BAT ligand (0.1 mmol, 100 mg) were removed by addition of 0.5 M HCl (2 mL) and heating at 100 °C for 20 min, followed by neutralization by addition of 0.1 M NaOH. To this solution, TBA[ReOCl<sub>4</sub>] (0.1 mmol, 59 mg) and NEt<sub>3</sub> (2 mmol, 0.25 mL) dissolved in methanol (10 mL) were added at 0 °C under a stream of nitrogen and the reaction mixture was stirred for 12 h at room temperature. The solvent was removed under reduced pressure. The residue was purified by preparative reversed phase high pressure liquid chromatography (RP-HPLC) on an XTerra column (10 μm, 10 mm × 250 mm; Waters) eluted with gradient mixtures of acetonitrile and water (0 min 20:80 V/V; 20 min 90:10 V/V) at a flow rate of 3 mL/min. UV detection was performed at 254 nm. Yield 7% (0.003 mmol, 2 mg). C<sub>16</sub>H<sub>25</sub>N<sub>4</sub>O<sub>4</sub>ReS<sub>3</sub> ESI-MS: [M + H]<sup>+</sup> calcd 619.7, found 619.9.

### 4.2.4. *S*-Benzylmercaptoacetylglucylglycine, *S*-Bn-MAG<sub>2</sub> (**4**)

The title compound was synthesized as previously reported by our group [29] with a yield of 71% as a white solid. C<sub>13</sub>H<sub>15</sub>N<sub>2</sub>O<sub>4</sub>SNa ESI-MS [M + Na]<sup>+</sup> calcd. 318.3, found 318.7.

### 4.2.5. Conjugation of AEBS with *S*-benzyl-MAG<sub>2</sub> (**5**)

The conjugation reaction was performed using similar reaction conditions as reported by Zhao et al. [30]. To a solution of 4-(2-aminoethyl)benzenesulfonamide (1.54 mmol, 308 mg) in 5 mL DMF, Bn-MAG<sub>2</sub> (1.54 mmol, 453 mg), DMAP (3.08 mmol, 375 mg) and PyBOP (3.08 mmol, 1.56 g) were added. The mixture was stirred overnight at room temperature and poured into 2 M HCl (50 mL)

saturated with NaCl. The white precipitate formed was filtered off, washed with water and recrystallized from ethanol/water, with a yield of 66% (1 mmol, 0.5 g) of a white solid.  $C_{21}H_{25}N_4O_5S_2Na$  ESI-MS:  $[M + Na]^+$  calcd 500.5, found 500.6.  $^1H$  NMR, 400 MHz (DMSO- $d_6$ )  $\delta$  8.29 (s, 1H), 8.18 (s, 1H), 7.91 (s, 1H), 7.73 (d, 2H,  $J = 7.96$  Hz), 7.38 (d, 2H,  $J = 7.88$  Hz), 7.24–7.31 (m, 6H,  $J = 3.89$  Hz), 3.81 (s, 2H), 3.74 (d, 2H,  $J = 5.16$  Hz), 3.66 (d, 2H,  $J = 5.28$  Hz), 3.36 (m, 3H), 3.11 (s, 2H), 2.79 (t, 2H,  $J = 6.66$  Hz).

#### 4.2.6. S-Benzoylmercaptoacetylglycylglycine (S-Bz-MAG<sub>2</sub>, **6**)

The title compound was synthesized as reported by our group [24] with a yield of 72%.  $C_{13}H_{13}N_2O_5SNa$  ESI-MS:  $[M + Na]^+$  calcd 332.3, found 332.6.

#### 4.2.7. Conjugation of AEBS with S-benzoyl-MAG<sub>2</sub> (**7**)

The conjugation was performed using a similar procedure as for the preparation of (**5**). To a solution of AEBS (308 mg, 1.54 mmol) in acetonitrile (20 mL) were added S-Bz-MAG<sub>2</sub> **6** (477 mg, 1.54 mmol), DMAP (375 mg, 3.08 mmol) and PyBOP (1.60 g, 3.08 mmol). DMF (2 mL) was added until a clear solution was obtained, and the mixture was stirred at room temperature for 4 days. The obtained white precipitate was filtered off, washed with water and recrystallized from methanol/water with a yield of 66% (1.1 mmol, 0.5 g).  $C_{21}H_{23}N_4O_6SNa$  ESI-MS:  $[M + Na]^+$  calcd 514.5, found 514.6.  $^1H$  NMR, 300 MHz (DMSO- $d_6$ )  $\delta$  8.56 (t, 1H,  $J = 5.68$  Hz), 8.19 (t, 1H,  $J = 5.3$  Hz), 7.91 (t, 3H,  $J = 7.4$  Hz), 7.71 (t, 3H,  $J = 9.2$  Hz), 7.56 (t, 2H,  $J = 7.5$  Hz), 7.37 (d, 2H,  $J = 8.0$  Hz), 7.30 (s, 2H), 3.90 (s, 2H), 3.77 (d, 2H,  $J = 5.3$  Hz), 3.66 (d, 2H,  $J = 5.5$  Hz), 3.17 (m, 2H,  $J = 6.0$  Hz), 2.77 (t, 2H,  $J = 7.0$  Hz).

#### 4.2.8. Complexation of **7** with rhenium (Re-**8**)

The complexation was carried out in 2 steps. In a first step, **7** (0.57 mmol, 280 mg) was deprotected by dissolving the product in 0.1 M NaOH (20 mL) and heating the solution for 10 min at 90 °C under N<sub>2</sub>. In a second step, rhenium (V) citrate was prepared by mixing sodium perrhenate (NaReO<sub>4</sub>, 0.4 mmol, 109 mg) and SnCl<sub>2</sub>·2H<sub>2</sub>O (0.4 mmol, 7.78 mg in 0.5 M citric acid (10 mL). This mixture was added to the solution of deprotected **7** obtained in the first step. The pH was adjusted to 10 by the addition of 0.1 M NaOH and the mixture was stirred for 1 h at 90 °C. After cooling to RT, (C<sub>6</sub>H<sub>5</sub>)<sub>4</sub>AsCl·H<sub>2</sub>O (20  $\mu$ mol, 8.7 mg) was added and the precipitate formed was filtered off and dried in vacuum. Yield 233 mg (0.4 mmol, 60%).  $C_{14}H_{16}N_4O_6S_2Re$  ESI-MS:  $[M + H]^+$  calcd 586.6, found 586.0.

#### 4.2.9. Conjugation of AEBS with N-BOC-L-Glu (BOC-Glu-bis-AEBS, **9**)

To a solution of N-BOC-L-Glu (1 mmol, 247 mg) in acetonitrile (150 mL) at 0 °C HOBT (2 mmol, 270 mg), EDC HCl (2 mmol, 383 mg) and AEBS (2 mmol, 400 mg) were successively added. The reaction mixture was stirred at 0 °C for 1 h and at RT for 72 h. The solvent was removed under reduced pressure and the residue was crystallized from a methanol-water mixture. Yield 540 mg (1 mmol, 100%).  $C_{26}H_{37}N_5O_8S_2$  calcd 611.7, found 611.8.  $^1H$  NMR, 400 MHz (DMSO- $d_6$ )  $\delta$  7.92 (Br s, 2H), 7.73 (m, 4H,  $J = 4.1$  Hz), 7.34 (m, 4H,  $J = 19.4$  Hz), 3.49 (signal overlap with H<sub>2</sub>O), 3.28 (m, 6H), 2.76 (m, 3H), 2.03 (Br s, 1H), 1.65 (m, 2H), 1.36 (s, 9H).

#### 4.2.10. Conjugation of BOC-Glu-bis-AEBS (**9**) with S-Bn-MAG<sub>2</sub> (**10**)

Under a stream of N<sub>2</sub>, TFA (1.5 mL) was added dropwise to a solution of **9** (0.25 mmol, 120 mg) in CH<sub>2</sub>Cl<sub>2</sub> (20 mL) at 0 °C and the solution was stirred for 4 h at RT. After removal of the solvent under reduced pressure, the residue was dissolved in toluene (5 mL) and the mixture concentrated to remove residual traces of TFA. A mixture of acetonitrile-DMF (10:1, 20 mL) was added, followed by **4**

(0.25 mmol, 70 mg), DMAP (0.5 mmol, 60 mg) and PyBOP (0.25 mmol, 260 mg). Stirring was continued at RT for 4 days. The obtained white precipitate was filtered off, washed with water and recrystallized from methanol-water to yield 70 mg (0.1 mmol, 36%) of a white solid.  $C_{34}H_{43}N_7O_6S_3$  ESI-MS:  $[M + H]^+$  calcd 789.2, found 789.2.  $^1H$  NMR, 400 MHz (DMSO- $d_6$ )  $\delta$  8.29 (m, 1H), 8.18 (m, 1H), 7.91 (m, 3H,  $J = 10.6$  Hz), 7.72 (m, 4H,  $J = 8.2$  Hz), 7.37 (m, 4H), 7.29 (m, 8H,  $J = 3.6$  Hz), 4.13 (m, 1H), 3.78 (m, 4H), 3.28 (m, 6H), 3.08 (m, 2H), 2.75 (m, 4H), 2.04 (m, 2H), 1.85 (s, 1H), 1.68 (m, 2H).

#### 4.2.11. $^{99m}Tc$ -BAT-AEBS; $^{99m}Tc$ -**3**

$^{99m}Tc$ -**3** was synthesized by a two-step one-pot reaction. In a first step, compound **2** (0.2 mg in 0.2 mL acetonitrile) and 0.5 M HCl (60  $\mu$ L) were mixed in a reaction vial which was heated at 100 °C for 20 min. After cooling down to RT, a cocktail solution (0.2 mL) consisting of buffering and chelating agents [0.5 M phosphate buffer pH 7.0 (5 mL), 0.1 M Na<sub>2</sub>EDTA (2.5 mL) and NaK tartrate (100 mg)] was added followed by addition of SnCl<sub>2</sub>·2H<sub>2</sub>O (0.015 mL of a 4 mg/mL solution in 0.05 M HCl) and  $^{99m}TcO_4^-$  solution (400–600 MBq/0.5 mL). The reaction mixture was heated at 100 °C for 10 min. After cooling to RT, an aliquot (0.5 mL) of the reaction mixture was purified by RP HPLC using system A.

#### 4.2.12. $^{99m}Tc$ -MAG<sub>2</sub>-AEBS; $^{99m}Tc$ -**8**

To a solution of compound **5** (0.5 mg/0.5 mL 0.5 M phosphate buffer, pH 8.0), NaK tartrate (10 mg, 0.25 mL in H<sub>2</sub>O), stannous chloride dihydrate (12 mg/mL in 0.05 M HCl, 25  $\mu$ L) and  $^{99m}TcO_4^-$  solution (400–600 MBq/0.5 mL) were added consecutively. The reaction mixture was heated at 100 °C for 15 min. After cooling to RT, an aliquot (0.5 mL) of the reaction mixture was purified by RP HPLC using system B. Radiochemical purity was assessed by RP HPLC (X Bridge™ C18 column, 3.5  $\mu$ m, 3 mm  $\times$  100 mm, Waters) at a flow rate of 0.6 mL/min.

#### 4.2.13. $^{99m}Tc$ -MAG<sub>2</sub>-Glu-bis-AEBS; $^{99m}Tc$ -**11A** and $^{99m}Tc$ -**11B**

The tracer agents were prepared according to the same procedure used for the preparation of  $^{99m}Tc$ -**8**. After cooling to RT, an aliquot (0.5 mL) of the reaction mixture was purified by RP-HPLC using system C.

#### 4.3. Log D<sub>1-octanol/phosphate buffer pH 7.4</sub> determination

Determination of the distribution coefficient was carried out by a shake flask method [31]. An aliquot (25  $\mu$ L) of  $^{99m}Tc$ -**5**,  $^{99m}Tc$ -**8** or  $^{99m}Tc$ -**11A** and  $^{99m}Tc$ -**11B** (185 kBq/mL) was added to a polypropylene tube (5 mL) (Sarstedt, Nümbrecht, Germany) containing 2 mL of 0.025 M sodium phosphate buffer pH 7.4 and 2 mL 1-octanol. The tubes were shaken for 2 min and then centrifuged at 3000 rpm for 10 min (Eppendorf centrifuge 5810, Eppendorf, Westbury, USA). Aliquots of 50  $\mu$ L 1-octanol and 500  $\mu$ L of phosphate buffer phases were pipetted out into separate tared eppendorf tubes with adequate care to avoid cross-contamination between the two phases. The samples were weighed and radioactivity was quantified using an automated gamma counter. The experiments were carried out six times.

#### 4.4. Inhibition studies (determination of $K_i$ )

The inhibition constants ( $K_i$ ) of the rhenium reference analogs Re-**3** and Re-**8** against hCA I, hCA II, hCA IX and hCA XII isozymes were determined by assaying the CA-catalyzed CO<sub>2</sub> hydration activity using an applied photophysics stopped flow instrument [32]. Phenol red (at a concentration of 0.2 mM) was used as indicator. The conditions included working at the absorbance maximum of 557 nm with 10 mM Hepes buffer (pH 7.5) and 0.1 M Na<sub>2</sub>SO<sub>4</sub> (for

maintaining constant ionic strength) and following the CA-catalyzed CO<sub>2</sub> hydration reaction for a period of 10–100 s. The CO<sub>2</sub> concentrations ranged from 1.7 to 17 mM for the determination of the kinetic parameters and inhibition constants at 25 °C. The uncatalyzed rates were determined in the same manner and subtracted from the total observed rates. Stock solutions of inhibitor (0.1 mM) were prepared in distilled water. Inhibitor (I) and enzyme (E) solutions were pre-incubated together for 15 min at room temperature prior to assay, this in order to allow for the formation of the E–I complex. The inhibition constants were obtained by non-linear least square methods using PRISM 3 (GraphPad Software, La Jolla, CA, USA) and represent the mean from at least three different determinations [33].

#### 4.5. Biodistribution studies

Colorectal (HT-29, ATCC HTB-38) adenocarcinoma cells were cultured as mentioned in our earlier report [19]. The cells were resuspended in Basement Membrane Matrix (Matrigel™ BD Biosciences, Breda, The Netherlands) and injected subcutaneously into the lateral flanks of NMRI – nu (nu/nu) mice. When the tumors reached an average volume of 400 mm<sup>3</sup> the mice were used for biodistribution studies. Each mouse received a dose of 0.1 MBq/0.15 mL of the tracers <sup>99m</sup>Tc-5, <sup>99m</sup>Tc-8 or <sup>99m</sup>Tc-11A and <sup>99m</sup>Tc-11B via a tail vein under isoflurane anesthesia (2% isoflurane in O<sub>2</sub> at 1 L/min flow rate). The mice were sacrificed by decapitation at 0.5, 1, 2 or 4 h post injection (p.i., *n* = 3/time point). Blood was collected and all major organs (heart, lungs, kidneys, liver, spleen, pancreas, brain, intestines, stomach and tumors) were excised and weighed. The radioactivity in each organ was quantified using a gamma counter, corrected for background radioactivity and expressed as percentage of the injected dose (% ID) or as percentage of the injected dose per gram tissue (% ID/g). For calculation of total radioactivity in blood, blood mass was assumed to be 7% of the total body mass.

#### 4.6. Western blot analysis

The validation of CA IX expression in the xenograft mice was carried out according to the procedure published by Dubois et al. [19]. Cells from the tumors were extracted in radio-immunoprecipitation assay (RIPA) buffer for 30 min on ice and protein concentrations were determined by a Bradford assay (Bio-Rad, Hercules, CA, USA) with bovine serum albumin (BSA) as standard. Proteins were separated on a 10% SDS–polyacrylamide gel (100 V, 1 h, 4 °C) and transferred to nitrocellulose membranes (Amersham Corp., USA). Membranes were blocked (2 h, RT) with 5% Blotting Grade Blocker non-fat dry milk (Bio-Rad) and subsequently incubated (overnight at 4 °C) with a 1:40 dilution of mouse monoclonal CA IX antibody M75 (kindly provided by Prof. Silvia Pastorekova, Institute of Virology, Slovak Academy of sciences, Bratislava, Slovak republic). Proteins were visualized by a horse-radish peroxidase method using Enhanced Chemiluminescence western blotting detection system (Amersham, Buckinghamshire, England). Mouse monoclonal β-actin (Cell Signaling Technology, Danvers MA, USA) was used as loading control.

#### 4.7. In vivo stability studies

The metabolic stability of the radiolabelled compounds <sup>99m</sup>Tc-5, <sup>99m</sup>Tc-8 or <sup>99m</sup>Tc-11A and <sup>99m</sup>Tc-11B was studied in normal NMRI mice (*n* = 2/time point) by determination of the relative amount of parent tracer and radiometabolites in plasma at 30 and 60 min p.i. After i.v. administration of about 3.7–6.3 MBq/0.2–0.3 mL of tracer via a tail vein under anesthesia (2% isoflurane in O<sub>2</sub> at 1 L/min flow

rate), the mice were decapitated and blood was collected at the above mentioned time points in lithium heparin containing tubes (4.5 mL LH PST tubes; BD vacutainer, Franklin Lakes, USA) and stored on ice. Next, the blood was centrifuged for 10 min at 3000 rpm to separate the plasma. The plasma (0.5 mL) was injected onto an HPLC system consisting of a Chromolith™ Performance column (3.0 mm × 100 mm, Merck), eluted with gradient mixtures of 0.01 M Na<sub>2</sub>HPO<sub>4</sub>, pH 8.0 (A) and acetonitrile (B) (0–4 min: 0% B, flow rate 0.5 mL/min; 4–20 min: linear gradient to 10% A and 90% B, flow rate 1 mL/min). The HPLC-eluate was collected as 1-mL fractions of which the radioactivity was measured using a gamma counter. The peak corresponding to the intact tracer was identified by comparing the retention time with the retention time of the intact tracers 9 and 10 analyzed on the same HPLC system.

#### Acknowledgments

We thank Peter Vermaelen and Ann Vansantvoort for excellent technical assistance and this work is supported by *in vivo* molecular imaging research (IMIR), K.U. Leuven, Belgium.

#### References

- [1] D. Neri, C.T. Supuran, Interfering with pH regulation in tumours as a therapeutic strategy, *Nat. Rev. Drug Discov.* 10 (2011) 767–777.
- [2] J. Bussink, J.H.Z.M. Kaanders, A.J. Kogel, Tumor hypoxia at the microregional level: clinical and predictive value of exogenous and endogenous hypoxic cell markers, *Radiother. Oncol.* 10 (2003) 3–15.
- [3] C. Trastour, E. Benizri, F. Ettore, A. Ramaioli, E. Chamorey, J. Pouyssegur, E. Berra, HIF-1α and CA IX staining in invasive breast carcinomas: prognosis and treatment outcome, *Int. J. Cancer* 120 (2007) 1451–1458.
- [4] V. Gregoire, K. Haustermans, X. Geets, S. Roels, M. Lonneux, PET-based treatment planning in radiotherapy: a new standard? *J. Nucl. Med.* 48 (2007) 68S.
- [5] J.M. Brown, W.R. Wilson, Exploiting tumour hypoxia in cancer treatment, *Nat. Rev. Cancer* 6 (2004) 437–447.
- [6] U. Koch, M. Krause, M. Baumann, Cancer stem cells at the crossroads of current cancer therapy failures–radiation oncology perspective, *Semin. Cancer Biol.* 2 (2010) 116–124.
- [7] S. Pastoreková, J. Pastorek, Cancer, related carbonic anhydrase isozymes and their inhibition, in: C.T. Supuran, A. Scozzafava, J. Conway (Eds.), *Carbonic Anhydrase: Its Inhibitors and Activators*, CRC Press, Boca Raton, FL, 2004, p. 255.
- [8] C.C. Wykoff, N.J.P. Beasley, P.H. Watson, K.J. Turner, J. Pastorek, A. Sibtain, G.D. Wilson, H. Turley, K.L. Talks, P.H. Maxwell, C.W. Pugh, P.J. Ratcliffe, A.L. Harris, Hypoxia-inducible expression of tumor-associated carbonic anhydrases, *Cancer Res.* 60 (2000) 7075–7083.
- [9] V. Alterio, M. Hilvo, A. Di Fiore, C.T. Supuran, P. Pan, S. Parkkila, A. Scaloni, J. Pastorek, S. Pastorekova, C. Pedone, A. Scozzafava, S.M. Monti, G. De Simone, Crystal structure of the catalytic domain of the tumor-associated human carbonic anhydrase IX, *Proc. Natl. Acad. Sci. U. S. A.* 106 (2009) 16233–16238.
- [10] G. De Simone, C.T. Supuran, Biochemical and crystallographic characterization of a novel antitumor target, *Biochim. Biophys. Acta* 1804 (2010) 404–409.
- [11] M. Ivan, K. Kondo, H. Yang, W. Kim, J. Valiando, M. Ohh, A. Salic, J.M. Asara, W.S. Lane, W.G. Kaelin, HIF1α targeted for VHL-mediated destruction by proline hydroxylation: implications for O<sub>2</sub> sensing, *Science* 292 (2001) 464–468.
- [12] C.T. Supuran, Carbonic anhydrases: novel therapeutic applications for inhibitors and activators, *Nat. Rev. Drug Discov.* 7 (2008) 168–181.
- [13] P. Swietach, S. Wigfield, C.T. Supuran, A.L. Harris, R.D. Vaughan-Jones, Cancer-associated, hypoxia-inducible carbonic anhydrase IX facilitates CO<sub>2</sub> diffusion, *BJU Int.* 101 (2008) 22–24.
- [14] B.A. Teicher, J.T. Liu, S.T. Liu, S.A. Holden, T.S. Herman, A carbonic anhydrase inhibitor as a potential modulator of cancer therapies, *Anticancer Res.* 13 (1993) 1549–1556.
- [15] M. Atkins, M. Regan, D. McDermott, J. Mier, E. Stanbridge, A. Youmans, P. Febbo, M. Upton, M. Lechhammer, S. Signoretti, Carbonic anhydrase IX expression predicts outcome of interleukin 2 therapy for renal cancer, *Clin. Cancer Res.* 11 (2005) 3714–3721.
- [16] A. Driessen, W. Landuyt, S. Pastorekova, J. Moons, L. Goethals, K. Haustermans, P. Naftaux, F. Penninckx, K. Geboes, T. Lerut, N. Ectors, Expression of carbonic anhydrase IX (CA IX), a hypoxia-related protein, rather than vascular-endothelial growth factor (VEGF), a pro-angiogenic factor, correlates with an extremely poor prognosis in esophageal and gastric adenocarcinomas, *Ann. Surg.* 243 (2006) 334–340.
- [17] C.R. Divgi, N. Pandit-Taskar, A.A. Jungbluth, V.E. Reuter, M. Gönen, S. Ruan, C. Pierre, A. Nagel, D.A. Pryma, J. Humm, S.M. Larson, L.J. Old, P. Russo, Pre-operative characterisation of clear-cell renal carcinoma using iodine-124

- labelled antibody chimeric G250 (124I-cG250) and PET in patients with renal masses: a phase I trial, *Lancet Oncol.* 8 (2007) 304–310.
- [18] J.R. Casey, P.E. Morgan, D. Vullo, A. Scozzafava, A. Mastrolorenzo, C.T. Supuran, Carbonic anhydrase Inhibitors. Design of selective, membrane-impermeant inhibitors targeting the human tumor-associated isozyme IX, *J. Med. Chem.* 47 (2004) 2337–2347.
- [19] L. Dubois, S. Peeters, N.G. Lieuwes, N. Geusens, A. Thiry, S. Wigfield, F. Carta, A. McIntyre, A. Scozzafava, J.M. Dogné, C.T. Supuran, A.L. Harris, B. Masereel, P. Lambin, Specific inhibition of carbonic anhydrase IX activity enhances the *in vivo* therapeutic effect of tumor irradiation, *Radiother. Oncol.* 99 (2011) 424–431.
- [20] V. Akurathi, L. Dubois, N.G. Lieuwes, S.K. Chitneni, B.J. Cleynhens, D. Vullo, C.T. Supuran, A.M. Verbruggen, P. Lambin, G. Bormans, Synthesis and biological evaluation of a 99mTc-labelled sulfonamide conjugate for *in vivo* visualization of carbonic anhydrase IX expression in tumor hypoxia, *Nucl. Med. Biol.* 5 (2010) 557–564.
- [21] S.M. Morsy, A.M. Badawi, A. Cecchi, A. Scozzafava, C.T. Supuran, Biphenylsulfonamides with inhibitory action towards the transmembrane, tumor-associated isozymes IX possess cytotoxic activity against human colon, lung and breast cancer cell lines, *J. Enzyme Inhib. Med. Chem.* (2009) 499.
- [22] G. Lu, S. Hillier, K. Maresca, C. Zimmerman, W. Eckelman, J. Joyal, J. Babich, Synthesis and SAR of novel Re/99mTc-labeled benzenesulfonamide carbonic anhydrase IX inhibitors for molecular imaging of tumor hypoxia, *J. Med. Chem.* 56 (2012) 510–520.
- [23] F. Jameel, S. Hershenson, Formulation and process development strategies for manufacturing biopharmaceuticals, in: J. Castner, P. Benites, M. Bresnick (Eds.), *Leachables and Extractables*, John Wiley & Sons, Inc, 2010, p. 857.
- [24] L. Hansen, L.G. Marzihi, D. Eshima, E.J. Malveaux, R. Folks, A. Taylor Jr., Evaluation of technetium-99m-triamide-mercaptide complexes designed to identify properties favoring renal tubular transport, *J. Nucl. Med.* 35 (1994) 1198–1205.
- [25] B.E. Gidal, G.L. Lensmeyer, Therapeutic monitoring of topiramate: evaluation of the saturable distribution between erythrocytes and plasma of whole blood using an optimized high-pressure liquid chromatography method, *Ther. Drug Monit.* 5 (1999) 567–576.
- [26] G. Anthoni, B. Langstrom, Molecular imaging I, in: *Handbook of Experimental Pharmacology*, vols. 185/1, II, Springer, 2008, pp. 177–201.
- [27] K. Serdons, T. Verduyck, J. Cleynhens, C. Terwinghe, L. Mortelmans, G. Bormans, A. Verbruggen, Synthesis and evaluation of a (99m)Tc-BAT-phenylbenzothiazole conjugate as a potential *in vivo* tracer for visualization of amyloid beta, *Bioorg. Med. Chem. Lett.* 17 (2007) 6086–6090.
- [28] T.N. Rao, D. Adhikesavalu, C. Arthur, A.R. Fritzberg, Synthesis and characterization of monooxorhenium(V) complexes of mercaptoacetylglycylglycylglycine. Crystal structure of tetrabutylammonium oxo(mercaptoacetylglycylglycylglycine)rhennate(V), *Inorg. Chim. Acta* 180 (1991) 63–67.
- [29] O.K. Hjelstuen, B.C. By, J. Cleynhens, H.M. Ormstad, T.E. Roald, H.H. Tonnesen, P.O. Bremer, A.M. Verbruggen, Comparative evaluation of 99mTc-MAG2-oligodeoxynucleotides with phosphodiester and phosphorothioate backbones: preparation; stability and biodistribution, *J. Labelled Compd. Radiopharm.* 42 (1999) 737–760.
- [30] Y.L. Zhao, C.L. Zhang, C.M. Qi, G.R. Feng, Z.L. You, F.G. Fu, R.F. Wang, Synthesis and biodistribution of 99mTc-peptides conjugated adenine as tumor imaging agents, *J. Radioanal. Nucl. Chem.* 273 (2007) 9–13.
- [31] H.P. Vanbilloen, K. Erates, N. Evens, C. Terwinghe, D. Rattat, G. Bormans, L. Mortelmans, A. Verbruggen, Preparation, characterization and biological evaluation of 99mTc(CO)<sub>3</sub>-labelled cyclic polyamines, *J. Labelled Compd. Radiopharm.* 48 (2005) 1003–1011.
- [32] R.G.T. Khalifah, The carbon dioxide hydration activity of carbonic anhydrase. I. Stop-flow kinetic studies on the native human isoenzymes B and C, *J. Biol. Chem.* 246 (1971) 2561–2573.
- [33] G. Bormans, B. Cleynhens, J. Hoogmartens, M. de Roo, A. Verbruggen, Evaluation of 99mTc-mercaptoacetyltri-peptides in mice and a baboon, *Int. J. Radiat. Appl. Instrum. B* 3 (1992) 375–388.